



Effect of Strike Deposition on Nanoscale Voiding in Electrolytic Ni/Au

Yeonseop Yu,^z Jinseok Kim, DoKyung Lim, SeongJae Lee, MiYang Kim, SangWon Lee, and JongSoo Yoo

Samsung Electro-Mechanics Company, Limited, Chungnam, Korea 339-702

Nanoscale voiding in electrolytic Ni/Au was studied by varying Au strike deposition conditions. Two kinds of voids were observed in electrolytic Ni/Au when electric current was not applied during strike plating. One was located along the interface between Ni and Au, which could deteriorate the adhesion between Ni and Au. The other was nanoscale bubbles coated with Ni inside Au film, which could result in porous Au layer. Our results suggest that Ni could grow on the surface of hydrogen bubbles and then the bubbles trapped in the Au film. Needlelike Au or Au whiskers were also observed on the Au surface and a line of nanoscale voids was found beneath Au whiskers when electric current was not applied during Au strike process. We propose a model that the nanoscale voiding and Au whisker formation could be related to a galvanic displacement reaction and hydrogen evolution at the early stage of Au electrodeposition.

© 2010 The Electrochemical Society. [DOI: 10.1149/1.3497293] All rights reserved.

Manuscript submitted January 25, 2010; revised manuscript received September 14, 2010. Published October 14, 2010.

Electrolytic Ni/Au surface finish has been commonly used in the electronic industry to provide both highly solderable and wire bondable surface for ball grid array packages. In particular, soft gold or pure gold is primarily used for connectors and printed circuits in which gold wire bonding of integrated circuits is required.¹⁻⁴ Electrolytic Ni is used as a undercoat prior to plating electrolytic Au and makes a good diffusion barrier for the base copper.

Electrolytic Ni and electrolytic Au processes employ galvanic electroplating which requires an applied electric current and a bus connection incorporated into the circuit design of the printed circuit board.⁵ The electric current increases the deposition rate and higher current usually provides a denser coating.

In a typical electrolytic Ni/Au process, there is a special plating process called "Au strike" or "Flash Au." Au strike process is used to form a very thin, typically less than 0.1 μm thick, plating with high quality and good adherence to the Ni substrate. Au strike plating serves as a foundation for subsequent Au plating process and plays an important role in securing the adhesion of the electroplated Au over Ni. When a Au film is lifted off the surface of Ni plating during gold wire bonding applications, the poor adhesion is frequently attributed to the Au strike process.

Au strike plating is usually performed in a bath with low concentration of the metal under high current density, which reduces galvanic displacement reactions. This is because the displacement reactions can be suppressed by lowering the electrode potential of metals given by

$$E = E^0 - \frac{RT}{nF} \ln \left(\frac{1}{M^{n+}} \right) \quad [1]$$

where E is the electrode potential, E^0 is the standard electrode potential, R is the universal gas constant, T is the absolute temperature, n is the number of electrons transferred, F is the Faraday constant, and M^{n+} is the concentration of the metal.

Although the Au strike process is widely used in industry and known to be responsible for the adhesion between Au and Ni in electrolytic Ni/Au, we do not completely understand how the very thin layer of Au strike can have a significant influence on the adhesion between Ni and Au. In the present study, we investigate the effect of Au strike deposit on the microstructure of electrolytic Ni and Au to understand the failure mechanism caused by poor adhesion.

Our finding is that improper Au strike plating is closely related to nanoscale voiding in electrolytic Ni/Au, which results in poor adhesion. On the basis of these results, we propose a model to explain the mechanism of voiding.

Experiments

In the present study, we followed a typical process sequence for deposition of electrolytic Ni and electrolytic Au, which includes acid clean, microetching, acid dip, Ni plating, Au strike, Au plating, rinse, and drying.

Ni was electroplated on a copper substrate in a nickel sulfamate bath operated at $50 \pm 5^\circ\text{C}$ and a pH of 4.0 ± 0.5 . The nickel sulfamate bath contained 450 ± 50 g/l nickel sulfamate, nickel chloride 12 ± 4 g/l, boric acid 25 ± 3 g/l, and proprietary additives. Au strike plating was carried out at $40 \pm 5^\circ\text{C}$ and a pH of 4.5 ± 0.5 for about 33 s in an aqueous solution containing 0.75 ± 0.25 g/l Au (as $\text{KAu}(\text{CN})_2$) with proprietary acid strike additives of JPC (Japan Pure Chemical, Tokyo, Japan). Au was then electrodeposited in a cyanide bath at $70 \pm 5^\circ\text{C}$ and a pH of 6.25 ± 0.15 for about 447 s. The concentration of Au was 5.0 ± 0.5 g/l as $\text{KAu}(\text{CN})_2$. Proprietary additive Tempersist EX (JPC) was used.

We deliberately did not apply an electric current during Au strike plating in the standard electroplating procedure in order to study the effect of Au strike plating on the microstructure of the electrodeposits.

The thicknesses of the Ni and Au were measured to be about 8 and 0.35 μm , respectively, from the cross-sectional focused ion beam (FIB) micrographs. We investigated the microstructure and composition of Ni and Au electrodeposits using a scanning electron microscopy (SEM) and X-ray photoelectron spectroscopy (XPS). We also employed a transmission electron microscope (TEM) equipped with an X-ray energy dispersive spectroscopy (EDS) detector and a high angle annular dark-field detector (HAADF). TEM specimens were prepared by using FIB operated at 30 kV. For these investigations, we used a Tecnai F20 S-TWIN TEM (FEI, Eindhoven, The Netherlands) operated at 200 kV, a Strata 400S dual-FIB (FEI, Eindhoven, The Netherlands), an S4800 SEM (Hitachi, Japan), and a Quantera XPS (PHI, USA).

Results and Discussion

We prepared two kinds of electrolytic Ni/Au surface finishes. One was prepared by the standard procedure described in the previous section, while the other sample was prepared without application of an electric current during Au strike plating.

Figure 1 shows the microstructures of electrolytic Ni/Au obtained from two kinds of samples. We can find striking differences between two samples, especially at the interface of Au and Ni. When no electric current was applied during Au strike, nanoscale voiding occurred at the interface and in the Au layer as marked by white and black arrows, respectively, as shown in Fig. 1b. Furthermore, the interface between Au and Ni is relatively rough compared to the sample prepared by the standard procedure. The voids at the interface do not have specific shape and are connected in some area. In

^z E-mail: yeonseop.yu@samsung.com

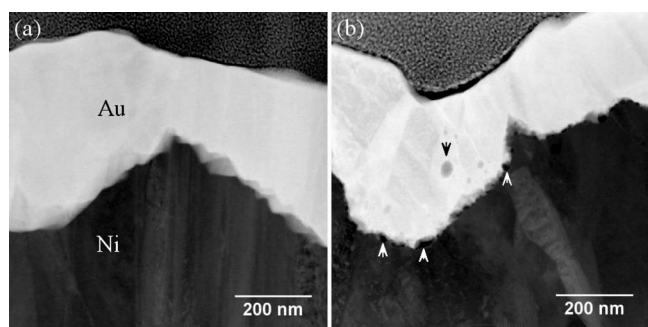


Figure 1. Cross-sectional HAADF STEM micrographs obtained from electrolytic Ni/Au prepared by Au strike plating (a) with application of an electric current and (b) without application of an electric current. The dark areas marked by the arrows are voids.

extreme case, a crack develops at the interface. On the other hand, the voids located in the Au electrodeposits are scattered in the Au layer in round shape and more frequently observed in the lower part of the Au layer.

Composition analysis across a void at the interface indicates that the void is deficient in Ni as shown in Fig. 2b. The void is not located in the middle of the interface, but right below the interface of Ni and Au if we assume that the interface is the crossing point of Ni and Au profiles as shown in Fig. 2. This suggests that Ni atoms should be dissolved into the plating solution to result in voiding. We confirm that the void is not filled with organic materials from image contrast and EDS analysis, which is not presented here.

We may suspect that nickel oxide (NiO) or nickel hydroxide (Ni(OH)₂) formation is responsible for the voiding at the interface. However, both XPS depth profile and chemical state analysis of Ni indicate that Ni is not oxidized but in metallic state at the interface as shown in Fig. 3.

There are some areas in which both Ni and Au exist at the top portion of the Ni layer near the interface as shown in Fig. 4a. The slightly bright particlelike features at the center in Fig. 4a are the areas where heavier element than Ni is present considering the Z-contrast of HAADF scanning transmission electron microscope (STEM) image. Composition profile across the interface clearly shows that they are Au-rich areas in the Ni layer right below the interface. Au can be found as far as about 150 nm below the interface in Fig. 4a. This finding again supports the idea that Ni is dissolved into the plating solution and Au is deposited in the area where Ni is dissolved out when no electric current is applied during Au strike.

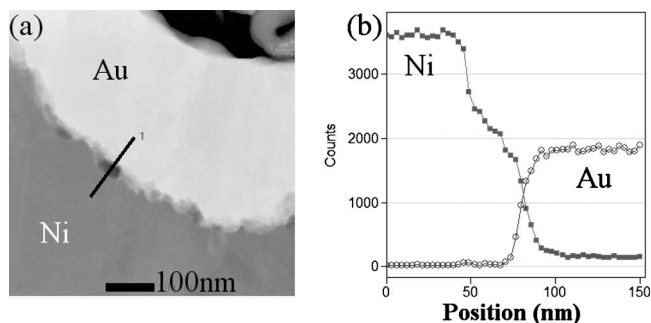


Figure 2. (a) Cross-sectional HAADF STEM micrograph showing voids at the interface of Au and Ni. (b) Compositional line profile across the interface of Au and Ni obtained from the line marked in (a). The region with low Ni concentration below the interface corresponds to the void located in the middle of the line marked in (a).

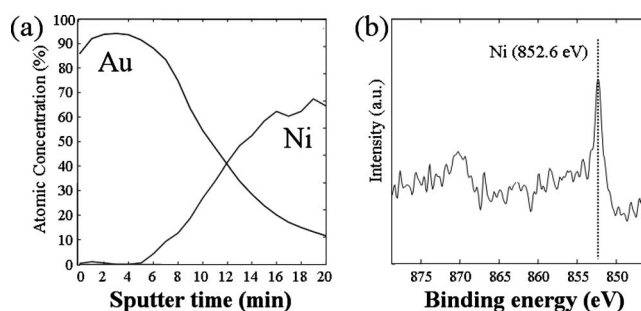
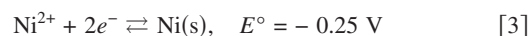
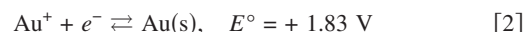


Figure 3. (a) XPS depth profile obtained from the electrolytic Ni/Au prepared by Au strike plating without an application of electric current. (b) XPS spectrum of Ni acquired from the interface of Au and Ni. It indicates that the Ni at the interface of Au and Ni is not nickel oxide but metallic Ni.

The nanoscale voiding at the interface and coexistence of Au and Ni right below the interface can be explained by galvanic displacement reactions caused by the difference in electrochemical potential for the Ni and Au as given by



The substrate Ni can be substituted with Au by the reaction $2\text{Au}^+ + \text{Ni}^0 \rightarrow 2\text{Au}^0 + \text{Ni}^{2+}$, instead of the electrolytic plating reaction by $\text{Au}^+ + e^- \rightarrow \text{Au}^0$ as depicted in Fig. 5. The dissolution of the Ni can lead to etching of Ni beneath the Au layer, which results in voids and thereby eventually makes the adhesion between Ni and Au weak.

The nanoscale voids in the Au layer are also of great interest since they can give some explanations on the origin of porosity of

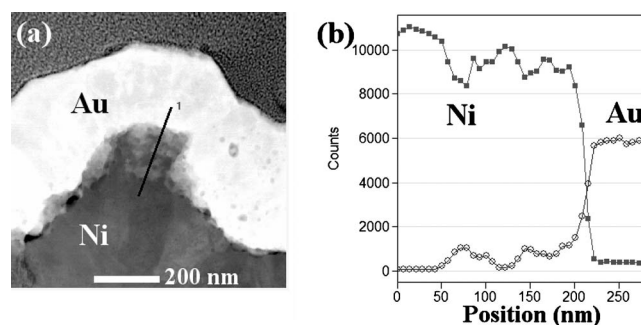


Figure 4. (a) Cross-sectional HAADF STEM micrograph showing the coexistence of Au and Ni below the interface of Au and Ni. (b) Compositional line profile across the interface of Au and Ni acquired from the line marked in (a). Au exists in the bright areas in the Ni layer below the interface.

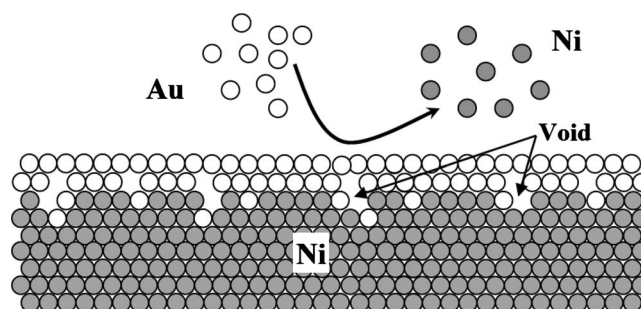


Figure 5. Schematic that shows the galvanic displacement reaction at the Ni and Au interface when electric current is not applied during Au strike plating. The white circles are Au and the gray circles represent Ni.

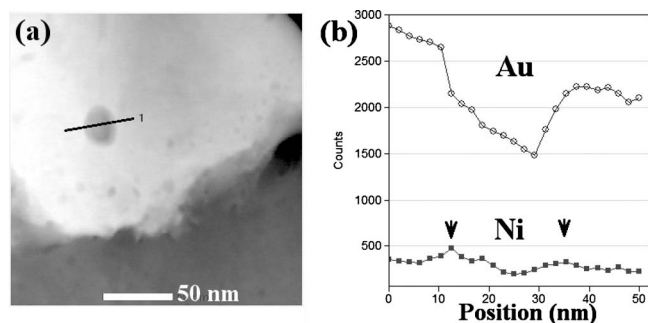


Figure 6. (a) Cross-sectional HAADF STEM micrograph showing the voids in the Au layer. (b) Compositional line profile across the void marked by the line in (a). The area with lower Au concentration in (b) corresponds to the void in (a). The locations marked by the arrows in (b) are the regions where Ni exist and correspond to the boundary of the void.

the Au electrodeposits. Unlike the voids in irregular shape observed at the interface between Ni and Au, the voids in the Au layer are in round shape. They look more like nanoscale bubbles of which size are less than 50 nm. The elemental analysis by EDS indicates that Ni exists in the voids in the Au layer as shown in Fig. 6b. Composition profile across the void in the Au layer clearly shows that the concentration of Ni is relatively high, especially, at the boundary of the void as marked by the arrows in Fig. 6b. Interestingly, the void is surrounded by a thin layer of Ni of which thickness is less than 10 nm in this particular case.

This observation can be related to the hydrogen bubbles that have been reported by many authors in metal electrodeposition.^{6,7} It is well known that hydrogen gas evolves at the cathode during electrodeposition as given by Eq. 4 or 5⁸



The dissolution of Ni mentioned above is not the only reaction that can occur at the interface of Ni and Au during Au strike. A small portion of electrons produced by dissolution of Ni in Eq. 3 and supplied by the power supply during Au electrodeposition can be consumed in the generation of hydrogen. The generated hydrogen gas can form bubbles on the Ni surface. This is a kind of alloy plating in which hydrogen is the codeposited element.

Nanoscale hydrogen bubbles in electrodeposits have been rarely observed, although microscale bubbles in electrodeposition coating have already been extensively studied due to their significant influence on the quality of the metal coating.^{9,10} Tsai et al. have shown that electrochemically generated hydrogen gas may lead to the formation of bubbles in electrodeposition and metal can grow directly on gas bubbles, leading to the formation of voids in the coating.⁹ Our observation of higher Ni concentration at the boundary of the voids suggests that Ni may grow on the surface of the hydrogen bubbles, which agrees well with the results of Tsai et al.

The voids in the Au layer can be explained by combining galvanic displacement reaction and hydrogen evolution during Au strike. Adopting the explanation of Hsu et al. on hydrogen bubbles and the growth of ramified zinc by electrodeposition,¹¹ the dissolved Ni ions in the electrolyte during Au strike are then reduced at the interface between the solution and the Ni surface, where the hydrogen bubbles do not occupy during electrolytic Au deposition. Due to the hydrogen bubbles on the Ni surface, the lateral growth of Ni and Au is suppressed, while the growth at the tip is accelerated by the concentrated electric field during electrolytic Au deposition. Hydrogen bubbles surrounded by a thin layer of Ni are then released from the Ni surface due to their buoyancy. This finally results in inclusions of hydrogen bubbles coated with Ni in the Au layer.

Another interesting observation related to the nanoscale voids in the Au layer is the needlelike features or whiskers existing on the Au

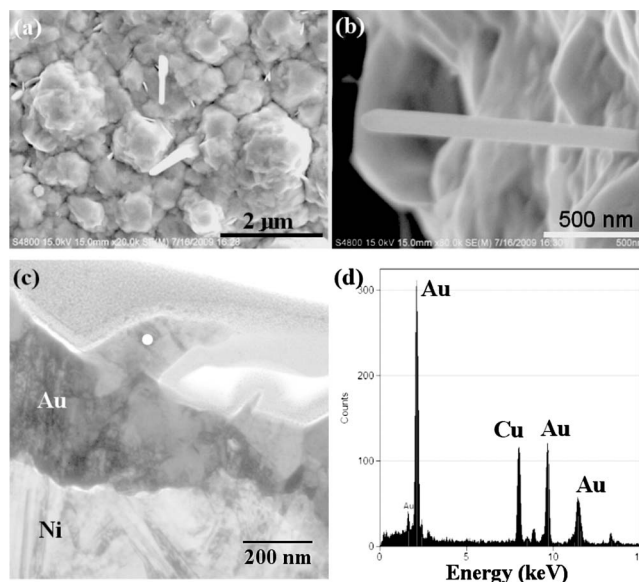


Figure 7. (a) SEM micrograph obtained from an electrolytic Ni/Au prepared by Au strike plating without application of electric current. It shows that needlelike features or whiskers exist on the Au surface. (b) Magnified image of a whisker. (c) Cross-sectional bright-field (BF) TEM micrograph showing a lower part of a whisker. The upper part of the whisker was lost during FIB milling. (d) An EDS spectrum obtained from the position in the Au whisker marked by the white circle in (c). It shows that the whisker consists of Au. Cu is detected due to use of a copper TEM grid.

surface as shown in Fig. 7a and b. The size of the whiskers is less than 200 nm in diameter and sometimes more than 1 μm in length. The image contrast of the bright-field TEM micrograph in Fig. 7c shows some grain structures in the whisker, and the EDS analysis indicates that the whisker consists of Au as shown in Fig. 7d. We can therefore conclude that the whiskers are polycrystalline Au.

Whisker formation in the electrodeposition of many metals such as Cu, Fe, and Ag have been known for decades.¹²⁻¹⁴ Whiskers of such metals were grown by adding some additives and controlling current densities. However, Au whiskers are very rare and we could find only one report by Teverovsky and Sharma from NASA.¹⁵ They have observed Au whiskers on the Au electrodeposits which were electroplated over the Ni electrodeposits. Their system is quite similar to ours. Typical whiskers observed by them have lengths of several micrometers and diameters of less than 200 nm, which are a little bigger than our observation. They have assumed that the whisker growth may be caused by the contamination of Au plating with rubidium during manufacturing.

In the present study, we have found some evidences that connect the Au whisker growth to nanovoiding. Although Au whiskers and the nanovoids in the Au electrodeposits do not seem to have any connection at first glance, it turns out that they are closely related. Figure 8a shows a Au whisker that is a small protrusion on the Au surface. Interestingly, a line of voids exists beneath the Au whisker as shown in Fig. 8a and b. Usually nanovoids in the Au electrodeposits existed at the lower part of the Au layer near the interface between Au and Ni as shown in Fig. 1b and 4a. However, we found that aligned nanoscale voids exist beneath the Au whiskers.

Furthermore, the dark area inside of the Au whisker is analyzed to be deficient in Au as shown in Fig. 8d. This indicates that the Au whisker has a sort of hollow structure at the bottom. If we combine two observations that a line of voids exists beneath the Au whiskers and there are voids at the bottom of Au whiskers, we can draw a hypothesis that the nanovoids result in Au whisker formation.

From our experimental results, a model for nanoscale hydrogen bubble formation, the growth of Ni on the surface of the bubbles, and Au whisker formation is devised as depicted in Fig. 9. This is

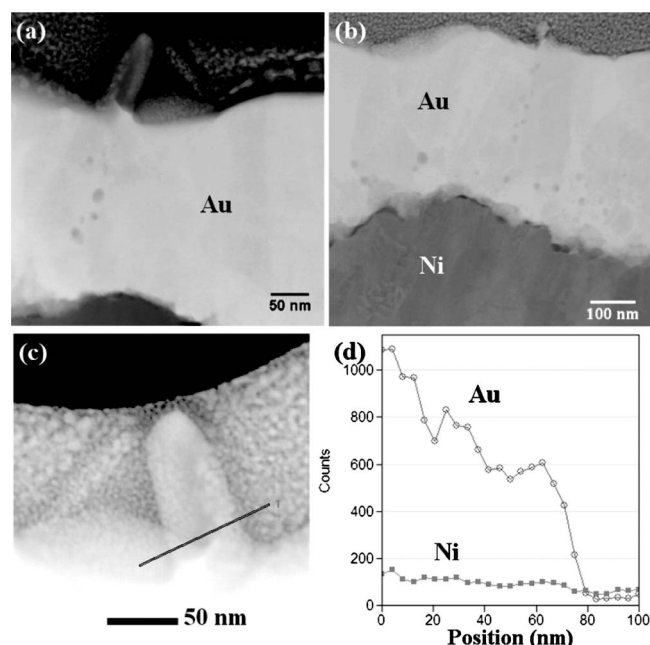


Figure 8. (a), (b) Cross-sectional HAADF STEM micrographs showing Au whiskers. Au whiskers are the protrusions on the Au surface. There are many voids below the Au whiskers. (c) Magnified image of the whisker shown in (a) and (d) Compositional line profile across the Au whisker marked by the line in (c). The center area of the line is deficient in Au. The concentration of Ni and Au is higher in the left because the whisker is overlapped with the Au layer. This can happen since we observe the projected image of a sample in TEM.

based on galvanic displacement reaction and accompanying hydrogen evolution. Hydrogen bubbles form and adhere to the Ni surface. Ni ions in the plating solution, which are displaced by Au, are deposited on the Ni surface which is not covered by hydrogen bubbles. As Ni electrodeposition proceeds, the hydrogen bubbles are covered by a thin layer of Ni. The bubbles may move during electroplating of Au until the Au film becomes dense, which results in permanent nanoscale voids. If the hydrogen bubbles covered with Ni can reach to the surface of the Au layer, electric field is concentrated on the bubbles, which results in Au whiskers.

Conclusion

If an electric current is not applied during Au strike plating, initial galvanic displacement reaction occurs during electrolytic Au plating. Ni is displaced by Au, which results in nanoscale voiding at the interface between Ni and Au. Furthermore, the displacement reaction is accompanied by hydrogen evolution which may form nanoscale bubbles. Ni can grow on the Ni surface which is not occupied by the bubbles and eventually surrounds the bubbles. These Ni-coated nanoscale bubbles can act as a seed for Au whisker formation during electrodeposition of Au.

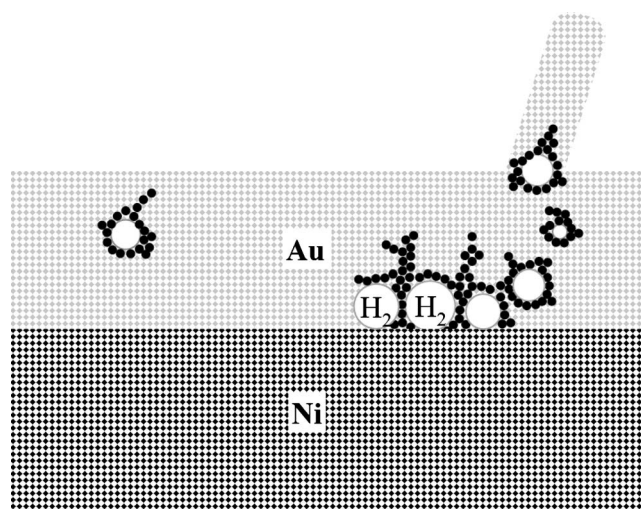


Figure 9. Schematic that shows hydrogen bubble formation and the growth of Ni on the surface of the bubbles. The white circles represent hydrogen bubbles and the black circles represent Ni. The protrusion on the Au surface represents a Au whisker.

We conclude that the adhesion between Ni and Au and the mechanical properties of the electrodeposits in electrolytic Ni/Au are closely connected to the displacement reaction and hydrogen evolution because those electrochemical reactions can generate nanoscale voids at the interface and in the Au film.

Samsung Electro-Mechanics Co., Ltd. assisted in meeting the publication costs of this article.

References

1. I. R. Christie and B. P. Cameron, *Gold Bull.*, **27**, 12 (1994).
2. Y. Okinaka and M. Hoshino, *Gold Bull.*, **31**, 3 (1998).
3. T. A. Green, *Gold Bull.*, **40**, 105 (2007).
4. J. Bath, *Lead-Free Soldering*, 1st ed., p. 250, Springer, Milpitas, CA (2007).
5. C. F. Coombs, Jr., *Printed Circuits Handbook*, 6th ed., p. 32.13, McGraw Hill Handbooks, New York (2007).
6. D. H. Coleman, B. N. Popov, and R. E. White, *J. Appl. Electrochem.*, **28**, 889 (1998).
7. M. Monev, L. Mirkova, I. Krastev, Hr. Tsvetkova, St. Rashkov, and W. Richtering, *J. Appl. Electrochem.*, **28**, 1107 (1998).
8. Cs. Szeles and A. Vertes, *J. Phys. F: Met. Phys.*, **17**, 2031 (1987).
9. W. L. Tsai, P. C. Hsu, Y. Hwu, C. H. Chen, L. W. Chang, J. H. Je, H. M. Lin, A. Growo, and G. Margaritondo, *Nature (London)*, **417**, 139 (2002).
10. L. Zhang, Y. Zhang, X. Zhang, Z. Li, G. Shen, M. Ye, C. Fan, H. Fang, and J. Hu, *Langmuir*, **22**, 8109 (2006).
11. P.-C. Hsu, S.-K. Seol, T.-N. Lo, C.-J. Liu, C.-L. Wang, C.-S. Lin, Y. Hwu, C. H. Chen, L.-. Chang, J. H. Je, et al., *J. Electrochem. Soc.*, **155**, D400 (2008).
12. P. A. van der Meulen and H. V. Lindstrom, *J. Electrochem. Soc.*, **103**, 390 (1956).
13. P. B. Price, D. A. Vermilyea, and M. B. Webb, *Acta Metall.*, **6**, 524 (1958).
14. A. V. Bondarenko, *Electrochim. Acta*, **29**, 887 (1984).
15. A. Teverovsky and A. Sharma, *SPIE: Micromachining and Microfabrication*, San Jose, CA, pp. 12–21 (2003).